Sr_3PbNiO_6: Trigonal Prismatic Lead in a Novel Inverse K_4CdCl_6-type Pseudo-One-Dimensional Oxide

Mark D. Smith,[†] Judith K. Stalick,[‡] and Hans-Conrad zur Loye*,[†]

Department of Chemistry and Biochemistry, University of South Carolina, Columbia, South Carolina 29208 and NIST Center for Neutron Research, National Institute of Standards and Technology, Gaithersburg, Maryland 20899

Received June 8, 1999. Revised Manuscript Received August 11, 1999

The new one-dimensional oxide Sr_3PbNiO_6 contains the first reported example of lead in the 2H hexagonal perovskite-related family of oxides with the formula $A_3A'BO_6$. The compound can be prepared by conventional high-temperature synthetic routes, or single crystals can be grown from a sodium chloride flux. Sr_3PbNiO_6 adopts the K_4CdCl_6 structure type ($R\bar{3}c$; $a = 9.7041(1)$ Å, $c = 11.3128(1)$ Å, $V = 922.59(1)$ Å^3, $Z = 6$), comprised of face-sharing polyhedral $^1_\infty[PbO_{6/2}NiO_{6/2}]$ chains surrounded by six $^1_\infty[Sr^{2+}]$ chains, both running along [001]. Pb^{4+} occupies a slightly distorted trigonal prismatic coordination environment previously unobserved in oxides; Ni^{2+} is octahedrally coordinated. The cation distribution in the polyhedral chains (+4 cation in the trigonal prismatic site, +2 in the octahedral site) is the inverse of that normally observed in the $A_3A'BO_6$ oxides. Sr_3PbNiO_6 is a Curie−Weiss paramagnet with an antiferromagnetic transition at $T_N = 6$ K. Complementary single-crystal and neutron diffraction structure determinations, thermogravimetric analysis, scanning electron microscopy, and magnetic susceptibility measurements are reported.

Introduction

Recently a host of pseudo-one-dimensional oxides with the formula $A_3A'BO_6$ has been reported (A = Ca, Sr, Ba; A′, B = metal, see below).[1−25] These oxides adopt the K_4CdCl_6 structure type,[26] and have proven quite attractive from a synthetic point of view due to their compositional flexibility. An impressive variety of magnetic and nonmagnetic A′ and B ions has been incorporated into the structure, including Li and Na,[2,15,21−22] Mg,[7] heavy main group ions (In, Bi),[13,22] and lanthanides,[4,7,12] in addition to the many transition metals which constitute the majority of the reported compounds. Oxidation states unusual in oxide chemistry are also stabilized in this structure type, for example Rh^{5+},[2] Ir^{5+},[14,15] and Ni^{3+}.[13] Such an adaptive structure type provides some experimental control over magnetic character, and indeed heightened investigation into this family of oxides has revealed a wealth of complex magnetic phenomena associated with their anisotropic structures, including random spin chain paramagnetism,[10] ferromagnetism,[12] antiferromagnetism,[4,17,19] and magnetic frustration.[3] The first structural systematization of this family was derived by Darriet and Subramanian in 1994,[27] who showed the relationship between these phases and the 2H hexagonal perovskites by conceiving of them as members of a larger family constructed from the hexagonal (...*ab*...) stacking of A_3O_9 (= 3 × AO_3) and $A_3A'O_6$ sheets (A = alkaline earth, A′

* To whom correspondence should be addressed.
† University of South Carolina.
‡ National Institute of Standards and Technology.

(1) Claridge, J. B.; Layland, R. C.; Henley, W. H.; zur Loye, H.-C. *Chem. Mater.* **1999**, *11*, 1376.
(2) Reisner, B. A.; Stacy, A. M. *J. Am. Chem. Soc.* **1998**, *120*, 9682.
(3) Claridge, J. B.; Layland, R. C.; Henley, W. H.; zur Loye, H.-C. *Z. Anorg. Allg. Chem.* **1998**, *624*, 1951.
(4) Kageyama, H.; Yoshimura, K.; Kosuge, K. *J. Solid State Chem.* **1998**, *140*, 14.
(5) Layland, R. C.; Kirkland, S. L.; zur Loye, H.-C. *J. Solid State Chem.* **1998**, *139*, 79.
(6) Aasland, S.; Fjellvag, H.; Hauback, B. *Solid State Commun.* **1997**, *101*, 187.
(7) Núñez, P.; Trail, S.; zur Loye, H.-C. *J. Solid State Chem.* **1997**, *130*, 35.
(8) Núñez, P.; Rzeznik, M. A.; zur Loye, H.-C. *Z. Anorg. Allg. Chem.* **1997**, *623*, 1269.
(9) Claridge, J. B.; Layland, R. C.; Adams, R. D.; zur Loye, H.-C. *Z. Anorg. Allg. Chem.* **1997**, *623*, 1131.
(10) Nguyen, T. N.; Lee, P. A.; zur Loye, H.-C. *Science* **1996**, *271*, 489.
(11) Lampe-Önnerud, C.; zur Loye, H.-C. *Inorg. Chem.* **1996**, *35*, 2155.
(12) Lampe-Önnerud, C.; Sigrist, M.; zur Loye, H.-C. *J. Solid State Chem.* **1996**, *127*, 25.
(13) James, M.; Attfield, J. P. *Chem. Eur. J.* **1996**, *2* 737.
(14) Frenzen, S.; Müller-Buschbaum, Hk. *Z. Naturforsch. B* **1996**, *51*, 225.
(15) Frenzen, S.; Müller-Buschbaum, Hk. *Z. Naturforsch. B* **1996**, *51*, 1204.
(16) Nguyen, T. N.; zur Loye, H.-C. *J. Solid State Chem.* **1995**, *117*, 300.
(17) Vente, J. F.; Lear, J. K.; Battle, P. B. *J. Mater. Chem.* **1995**, *5*, 1785.
(18) Frenzen, S.; Müller-Buschbaum, Hk. *Z. Naturforsch. B* **1995**, *50*, 581.
(19) Nguyen, T. N.; Giaquinta, D. M.; zur Loye, H.-C. *Chem. Mater.* **1994**, *6*, 1642.
(20) Tomaszewska, A.; Müller-Buschbaum, Hk. *Z. Anorg. Allg. Chem.* **1993**, *619*, 534.
(21) Wehrum, G.; Hoppe, R. *Z. Anorg. Allg. Chem.* **1992**, *617*, 45.
(22) Carlson, V. A.; Stacy, A. M. *J. Solid State Chem.* **1992**, *96*, 332.
(23) Tomaszewska, A.; Müller-Buschbaum, Hk. *Z. Anorg. Allg. Chem.* **1992**, *617*, 23.
(24) Neubacher, M.; Müller-Buschbaum, Hk. *Z. Anorg. Allg. Chem.* **1992**, *607*, 124.
(25) Wilkinson, A. P.; Cheetham, A. K.; Kunnman, W.; Kvick, Å. *Eur. J. Solid State Inorg. Chem.* **1991**, *28*, 453.
(26) Bergerhoff, G.; Schmitz-Dumont, O. *Z. Anorg. Allg. Chem.* **1956**, *284*, 10.
(27) Darriet, J.; Subramanian, M. *J. Mater. Chem.* **1995**, *5*, 543.

10.1021/cm990360p CCC: $18.00
Published on Web 09/18/1999

= metal). The latter sheet is easily derived from a perovskitic A_3O_9 sheet by substitution of a heterocation A′ for three adjacent oxide ions. The general formula derived in this fashion is $A_{3n+3}A'_nB_{n+3}O_{6n+9}$; the B cation arises from filling of the octahedral interstices between stacked close-packed sheets. In this scheme, the n value represents the ratio of $A_3A'O_6$ sheets to A_3O_9; thus, n = 0 yields the ABO_3 (hexagonal) perovskites, composed solely of AO_3 sheets and containing chains of face-shared $NiO_{6/2}$ octahedra separated by A cations. The other endmember, $n = \infty$, generates the composition $A_3A'BO_6$, composed solely of $A_3A'O_6$ sheets, and contains chains of alternating (and slightly distorted) $A'O_{6/2}$ trigonal prisms and $BO_{6/2}$ octahedra which share faces along the hexagonal c axis. These chains are then surrounded by six chains of A^{2+} cations. Intermediate values of n correspond to varying sheet sequences and give rise to different ratios of trigonal prisms and octahedra along the $^1_\infty[A'O_{6/2}BO_{6/2}]$ polyhedral chains.

While these compounds have appealed to various groups because of their amenability to the study of pseudo one-dimensional magnetic phenomena, another area of interest is expanding the range of elements that can be incorporated into the metal−oxygen polyhedral chain. Thus far, the $n = \infty$ homologue ($A_3A'BO_6$) has proven the most fruitful and receptive stoichiometry and is exemplified by numerous A′ and B cations pairs in the oxidation state combinations +1/+5 (e.g., Sr_3(Li,Na)RhO_6, Ba_3NaRuO_6),[2,15] +2/+4, (e.g., $Ca_{4-x}Ni_xIrO_6$, Sr_3CuPtO_6),[3,25] and +3/+3 (e.g., Sr_3GdRhO_6, Sr_3YbNiO_6).[8,13] To our knowledge, no +4/+2 couple has been reported. Investigation into the Sr−Pb−Ni−O system has led to our discovery of Sr_3PbNiO_6, an unprecedented "inverse" K_4CdCl_6-type oxide featuring Pb^{4+} in a heretofore unobserved near-trigonal prismatic coordination environment (the A′ site) and also containing the first example of Ni^{2+} on the octahedral B site of the $A_3A'BO_6$ structure. This cation distribution is the inverse of the usual observation of a trigonal prismatic +2 cation and an octahedral +4 cation in this structure. Herein we report the synthesis and characterization of Sr_3PbNiO_6, a novel addition to this rich family of oxides.

Experimental Section

Synthesis. Sr_3PbNiO_6 is best made by a metal acetate coprecipitation precursor route: Stoichiometric amounts of Sr(OAc)$_2$ (Aesar, 99.99%), Ni(OAc)$_2$·4H$_2$O (Johnson-Mathey, reagent), and Pb(OAc)$_2$·3H$_2$O (Alfa, 99.99%) were dissolved in deionized water. The water was evaporated (boiled off), and the light green powder ground finely before calcining at 650 °C for 12 h. The dark powder was then subjected to the following heat treatment, always with intermediate grinding/pellet pressing: 650 °C, 6 h; 850 °C, 12 h; 1050 °C, 24 h; 1050 °C, 24 h; 1050 °C, 18 h. Polycrystalline Sr_3PbNiO_6 is reddish-brown in color and is stable indefinitely in air. Alternately, the compound can be made by direct reaction of intimately mixed and pelletized $SrCO_3$, PbO_2 (or PbO), and NiO at 1050 °C with five to six one-day grind−pelletize−fire cycles. The Sr_3PbNiO_6 prepared this way is more prone to contamination with Sr_2PbO_4 and NiO than acetate precursor samples.

Small single crystals of Sr_3PbNiO_6 can be grown from a sodium chloride flux, using presynthesized Sr_3PbNiO_6 as the precursor. An alumina crucible is charged with a 1:10 by mass mixture of Sr_3PbNiO_6/NaCl (typical charge: 1 g Sr_3PbNiO_6, 10 g NaCl), covered, heated to 1000 °C for 24h, and then slow-cooled to 750 °C at 50 °C/h, whereupon the furnace is turned off and allowed to cool radiatively to room temperature. The NaCl flux matrix is easily removed by dissolution in water, leaving unnucleated powder and black faceted blocks in approximately equal proportions. The single crystals (typical dimensions: polycrystalline to 0.15 mm) are distributed uniformly on the crucible walls and embedded in the powder remaining on the crucible bottom.

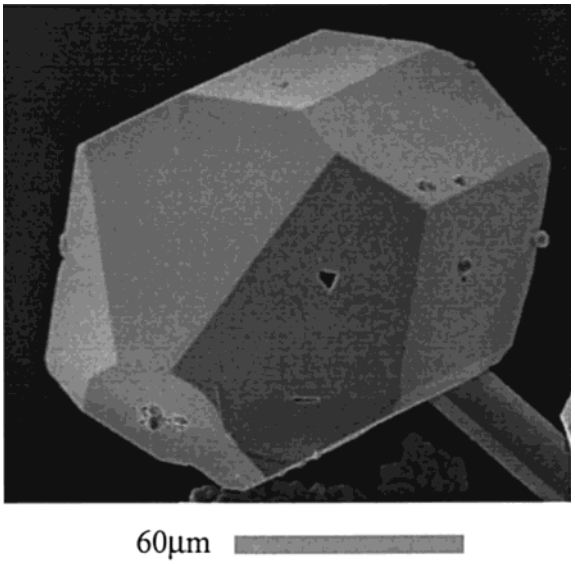

Figure 1. Single crystal of Sr_3PbNiO_6 grown from a NaCl flux.

Table 1. Single-Crystal Data for Sr_3PbNiO_6

formula weight	624.76
crystal system	rhombohedral (hexagonal setting)
space group	$R\bar{3}c$
lattice parameters (Å)	
a	9.7055(5)
c	11.3120(5)
volume (Å^3)	922.80(8)
Z	6
density (calcd)	6.745 g/cm^3
refinement method	full matrix least-squares on F^2
data/parameters	593/19
R values[a] ($I > 2\sigma(I)$)	R1 = 0.0299; wR2 = 0.0653
R values[a] (all data)	R1 = 0.0395; wR2 = 0.0678
goodness-of-fit (F^2)	1.064
largest diff. peak and hole	7.753; −2.564 e$^-$/Å^3

[a] $R1 = \Sigma||F_o| - |F_c||/\Sigma|F_o|$; $wR2 = \{\Sigma[w(F_o^2 - F_c^2)^2]/\Sigma[w(F_o^2)^2]\}^{1/2}$; $w = 1/\sigma^2(F_o^2)$.

Scanning Electron Microscopy. Scanning electron micrographs of several single-crystal samples were obtained using a Hitachi 2500 Delta SEM instrument. The crystals were sputtered with gold to prevent charging. An SEM image of a typical crystal is shown in Figure 1. The SEM also verified the presence of Sr, Pb, and Ni in all crystals. No Na or Cl (from the flux) was detected.

Single-Crystal Structure Determination. A small black prismatic crystal grown from the NaCl flux was epoxied onto a glass fiber (approximate crystal dimensions 0.015 × 0.015 × 0.020 mm). X-ray intensity data were measured at 293 K on a Bruker SMART 1000 CCD-based diffractometer equipped with Mo radiation (λ = 0.71073 Å). The crystal-to-detector distance was 2.900 cm. A total of 1868 frames of data were collected with a scan width of 0.3° in ω, giving a total of 6829 reflections ($2\theta_{max}$ = 78.11°), of which 593 were unique (redundancy 11.51, completeness = 98.5%, R_{int} = 5.93%), and 492 with $F > 4\sigma(F)$. The final cell constants (see Table 1) were based upon the refinement of 3153 reflections with $I > 2\sigma(I)$. The crystal showed negligible decay during data collection. Data were corrected for absorption effects using the SADABS program, with minimum and maximum transmission coefficients of 0.510 and 0.928, respectively, and μ = 56.089 mm^{-1}. The structure was solved and refined using SHELXTL. Further details of the solution are presented in Table 1. While

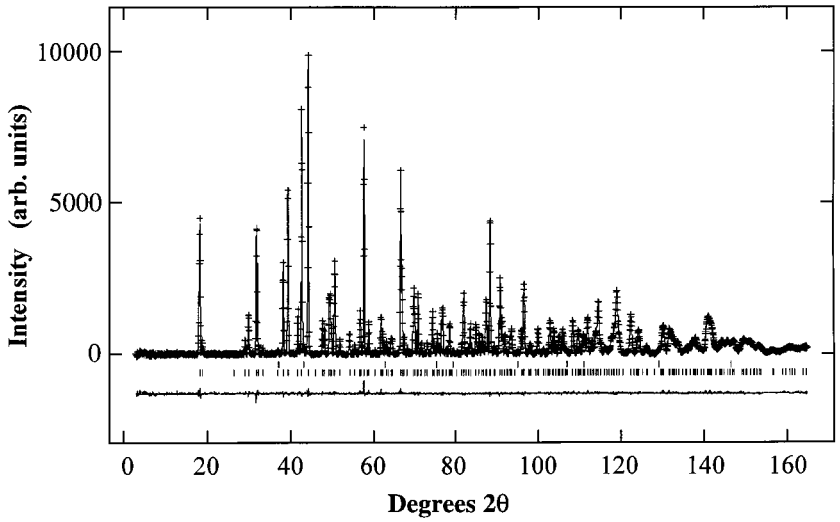

Figure 2. Observed (+) and calculated (solid line) neutron powder diffraction pattern for Sr_3PbNiO_6, with difference plot (observed − calculated) obtained from the Rietveld refinement (bottom). The lower set of tick marks represents the allowed Bragg reflections for Sr_3PbNiO_6; the upper tick marks, for NiO.

the X-ray diffraction measurement conclusively determined the distribution of metal atoms on their respective crystallographic sites, the atomic positions of the light (oxygen) atoms derived from these data are less certain. To provide more accurate oxygen atomic positions, as well as to corroborate the single-crystal structure determination, a powder neutron diffraction study was carried out.

Neutron Powder Diffraction. Room-temperature neutron diffraction data on 6.0 g of Sr_3PbNiO_6 contained in a $^3/_8$-in.-diameter vanadium sample can were collected using the BT-1 32-detector high-resolution neutron powder diffractometer at the National Institute of Standards and Technology Center for Neutron Research, Gaithersburg, MD. The neutron wavelength was 1.5402(1) Å. Data from the 32 detectors were combined to give pseudo-one-detector data over a total scan range of $3° \le 2\theta \le 168°$. The structure was solved by Rietveld[28] refinement (as implemented in the GSAS[29] suite of programs) using information from the single-crystal solution as a structural model. The neutron diffraction data reproduced the single-crystal X-ray diffraction data in all respects; however, since the neutron scattering lengths of Pb and Ni are very similar (9.4 and 10.3 fm, respectively), these atoms are best distinguished by the X-ray data. During the refinement, a minor nickel oxide impurity was detected (0.4 wt %). Due to the efficacy of nickel as a neutron scatterer, including NiO in the refinement lowered the χ^2 value from 3.25 to 1.25, justifying the two-phase refinement. The neutron diffraction pattern with difference plot (observed − calculated) is shown in Figure 2. Upper tick marks correspond to the allowed NiO Bragg reflections; the lower to those for Sr_3PbNiO_6. Rietveld and least-squares refinement results, atomic coordinates and thermal parameters, and selected bond distances and angles are presented in Tables 2, 3 and 4, respectively. The bond distances and angles derived from the single-crystal and neutron diffraction data are identical within experimental error, and therefore only the neutron results are presented.

Thermogravimetric Analysis. A sample of Sr_3PbNiO_6 was heated to 850 °C under in a stream of 5% H_2 in N_2 at a flow rate of 5 mL/min, using a TA Instruments SDT 2960 simultaneous DTA-TGA. A weight loss was observed (onset 400 °C, complete by 650 °C) corresponding to the process $Sr_3PbNiO_6 + 3H_2\,(g) \rightarrow 3SrO + Pb + Ni + 3H_2O\,(g)$ (calcd 7.68%, meas 7.66%). The identity of the residue (SrO, Pb, Ni) was confirmed by X-ray powder diffraction.

Magnetic Susceptibility. Magnetic susceptibility of Sr_3PbNiO_6 as a function of temperature was measured using a Quantum Design MPMS XL SQUID magnetometer, at applied field strengths of 5 and 40 kOe. Both field-cooled (FC) and zero-field cooled (ZFC) measurements were performed, in the temperature range $2\ K \le T \le 300\ K$. The sample (509.3 mg) was contained in a gelatin capsule fastened in a plastic straw for immersion into the SQUID. No diamagnetic correction was made for the sample container.

Table 2. Neutron Powder Diffraction Rietveld Refinement Results for Sr_3PbNiO_6

space group	$R\bar{3}c$
lattice parameters (Å)	
a	9.7041(1)
c	11.3128(1)
volume (Å^3)	922.59(1)
no. reflections	248
no. refined parameters	35
R_p[a]	0.0271
wR_p[a]	0.0330
R_{exp}[a]	0.0297
R_{Bragg}[a]	0.0137
χ^2	1.25

[a] $R_p = [\sum|I_o - I_c|/\sum I_o]$; w$R_p = [\sum w(I_o - I_c)^2/\sum wI_o^2]^{1/2}$; $R_{exp} =$ w$R_p/[(\chi^2)^{1/2}]$ $R_{Bragg} = [\sum|I_{k(obs)} - I_{k(calc)}|/\sum I_{k(obs)}]$. I_o and I_c are observed and calculated intensities, respectively; w is a weight derived from an error propagation scheme during the refinement process, and I_k is the Bragg intensity

Table 3. Atomic Coordinates and Isotropic Thermal Parameters (U_{iso}), from Rietveld Refinement of the Neutron Diffraction Data

atom	site	x	y	z	U_{iso}
Sr	18e	0.37232(6)	0	0.25	0.0082(1)
Pb	6a	0	0	0.25	0.0058(2)
Ni	6b	0	0	0	0.0064(1)
O	36f	0.17617(5)	0.02053(5)	0.11694(4)	0.0086(1)

Table 4. Bond Distances and Angles Derived from Rietveld Refinement of the Neutron Diffraction Data

bond	distance (Å)	atom	atom	atom	angle (deg)
Sr−O	2.512(1) (×2)	Pb	O	Ni	86.16(2)
Sr−O	2.681(1) (×2)	O	Pb	O	78.73(2)
Sr−O	2.682(1) (×2)	O	Pb	O	145.50(2)
Pb−O	2.211(1) (×6)	O	Ni	O	84.23(2)
Ni−O	2.091(1) (×6)	O	Ni	O	95.77(2)
		O	Ni	O	180.00

(28) Rietveld, H. M. *J. Appl. Crystallogr.* **1969**, *2*, 65.

(29) Larson, A. C.; Von Dreele, R. B. General Structure Analysis System (GSAS). Los Alamos National Laboratory, 1994; Report No. LA-UR-86-748.

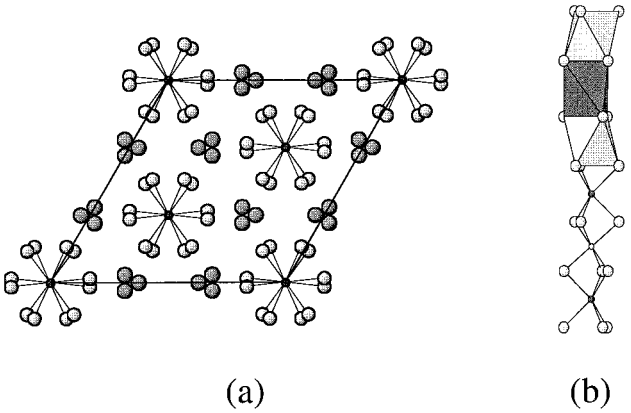

Figure 3. (a) [001] view of Sr_3PbNiO_6 (small dark circles, Ni or Pb; large dark circles, Sr; large gray circles, O) and (b) section of a $^1_\infty[PbO_{6/2}NiO_{6/2}]$ chain (dark gray indicates Pb atoms or $PbO_{6/2}$ trigonal prisms; light gray, nickel atoms or $NiO_{6/2}$ octahedra).

Results and Discussion

Sr_3PbNiO_6 adopts the K_4CdCl_6 structure type, consisting of chains of face-shared $^1_\infty[PbO_{6/2}NiO_{6/2}]$ metal−oxygen polyhedra running parallel to [001]. These chains are separated and charge-balanced by $^1_\infty[Sr^{2+}]$ chains surrounding the metal−oxygen chains in a hexagonal fashion. In fact, these $^1_\infty[Sr^{2+}]$ chains form a Kagomé-like net pattern, the large voids of which are occupied by the metal−oxygen chains. Figure 3a shows a [001] view of the structure. In the Darriet−Subramanian scheme discussed earlier, Sr_3PbNiO_6 is an $n = \infty$ member of the $A_{3n+3}A'_nB_{n+3}O_{6n+9}$ family, constructed by stacking all $A_3A'O_6$ (i.e., Sr_3PbO_6) sheets and no A_3O_9 (Sr_3O_9) sheets. This generates a metal−oxygen polyhedron sequence of strictly alternating trigonal prisms and octahedra (1:1 ratio), which share faces and propagate along the crystallographic [001] direction. In Sr_3PbNiO_6, the trigonal prismatic sites are occupied by Pb^{4+} ions, with six equivalent Pb−O distances of 2.211(1) Å, and the octahedral sites are occupied by Ni^{2+} ions, with Ni−O (×6) = 2.091(1) Å. The Sr^{2+} ions occupy an irregular eight-coordinate site (local point symmetry C_2) consisting of six oxygen atoms from two $NiO_{6/2}$ octahedra and two from other octahedra, with Sr−O distances in the range 2.512(1) − 2.687(1) Å. (All reported bond distances derived from the neutron data.) Although lacking a Pb^{4+} ion in a similar coordination environment with which to compare, these Pb−O distances are close to those reported for octahedral Pb^{4+} in the perovskite-related phase $SrPbO_3$ (2.157 and 2.165 Å);[30] the Ni−O distances agree well with those in octahedrally coordinated NiO (2.089 Å).[31] The Sr−O distances are typical of those in other $Sr_3A'BO_6$ compounds.[1] Figure 3b shows a section of a $^1_\infty[PbO_{6/2}NiO_{6/2}]$ chain, illustrating the coordination polyhedra around the metal ions. (Although loosely referred to as "trigonal prismatic" and "octahedral", both polyhedra are actually slightly distorted, as follows: the opposite triangular faces of the $PbO_{6/2}$ trigonal prism are twisted by 12.2° relative to one another, and the $NiO_{6/2}$ octahedra are rhombohedrally elongated with O−Ni−O angles of 95.8° and 84.2°.)

The Pb^{4+} ion has been reported in varied coordination geometries in oxides, including tetrahedral,[32] trigonal bipyramidal,[33] and square pyramidal.[34] Of course, examples of octahedral Pb^{4+} are quite common. However, Sr_3PbNiO_6 represents, to our knowledge, the first example of a trigonal prismatically coordinated Pb^{4+} ion in an oxide. Indeed, Sr_3PbNiO_6 can be considered to contain the third distinct coordination mode observed for lead in lead-containing perovskites. In the cubic and cubic-derived perovskites ABO_3, divalent lead is well-known to occupy the 12-coordinate "A" site in compounds such as $PbMO_3$ (M = Ti, Zr, Hf),[35] and, as Pb^{4+}, to occupy the octahedral B-site in $APbO_3$ (M = Ca, Sr, Ba)[36] and in double perovskites such as A_2MPbO_6 (M = Ce, Pr, Tb).[37] It should be noted that although Sr_3PbNiO_6 is the first lead-containing $A_3A'BO_6$ compound, the K_4CdCl_6-type halides Cs_4PbX_6 (X = Cl, Br, I) are known.[38] In these compounds lead occupies the octahedral B site as the +2 cation.

In general, the distribution of A′ and B site oxidation states in the $A_3A'BO_6$ oxides is +1/+5, +2/+4, or +3/+3, respectively, and many examples of each are known. Sr_3PbNiO_6 is the first observation of a +4/+2 system, and so by analogy to the categorization of "normal" and "inverse" spinels based on the distribution of cation oxidation states on the crystallographic sites, we suggest the term "inverse" to describe this new compound. The site preference in the polyhedral chains can be correlated with cation size: the trigonal prism volume is larger than the octahedron volume, since it in theory replaces two octahedra in the chains. Consequently a larger cation is more suitable in this site. In fact, no $A_3A'BO_6$ compounds are known where the radius of the cation in the trigonal prismatic A′ site is smaller than the radius of the cation in the B site; the nearest to an exception to this is Ba_3LiBiO_6,[22] where the radii of Li^+ and Bi^{5+} are identical (0.76 Å).[39] Sr_3PbNiO_6 contains a large sixth-row main group ion (Pb^{4+} six-coordinate radius = 0.78 Å) and a small first-row transition metal ion (Ni^{2+} six-coordinate radius = 0.69 Å).[39] Apparently, this propitious distribution of metal radii (a tetravalent cation larger than a divalent cation) permits this novel "inverse" cation distribution.

The occurrence of Ni^{2+} in the octahedral site of an $A_3A'BO_6$ oxide is also unusual. Several examples of Ni^{2+} in the trigonal prismatic site in these compounds are known, most obviously A_3NiMO_6 (A = Ca, Sr; M = Pt, Ir).[1,3,16] James and Attfield have reported Ni^{3+} in the octahedral B site in the compounds Sr_3MNiO_6 (M = Sc, In, Lu, Yb, Tm).[13] Additionally, octahedral Ni^{4+} occurs in the 2H hexagonal perovskites $ANiO_3$ (A = Sr, Ba).[40]

Sr_3PbNiO_6 shows nearly ideal Curie−Weiss behavior above ~20 K (Figure 4), with $\mu_{eff} = 2.91\ \mu_B$, in excellent

(30) Fu, W. T.; Ijdo, D. J. W. *Solid State Commun.* **1995**, *95*, 581.
(31) Sasaki, S.; Fujino, K.; Takeuchi, Y. *Proc. Jpn. Acad.* **1979**, *55*, 43.
(32) Brandes, R.; Hoppe, R. *Z. Anorg. Allg. Chem.* **1994**, *620*, 1346.
(33) Brazel, B.; Hoppe, R. *Z. Anorg. Allg. Chem.* **1983**, *497*, 176.
(34) Stoll, H.; Hoppe, R. *Z. Anorg. Allg. Chem.* **1987**, *551*, 151.
(35) West, A. R. *Solid State Chemistry*; John Wiley & Sons: New York, 1984.
(36) (a) Yamamoto, A.; Khasanova, N.; Wu, X.-J.; Tanabe, K. *Solid State Ionics* **1998**, *108*, 333. (b) Shannon, R. D.; Bierstedt, P. E. *J. Am. Ceram. Soc.* **1970**, *53*, 635.
(37) Harrison, W. T. A.; Reis, K. P.; Liu, L. M.; Jacobson, A. J. *Mater Res. Bull.* **1995**, *30*, 1455.
(38) Greenwood, N. N.; Earnshaw, A. *Chemistry of the Elements*; Pergamon: Elmsford, NY, 1984; p 445.
(39) Shannon, R. D. *Acta Crystallogr.* **1976**, *A32*, 751.

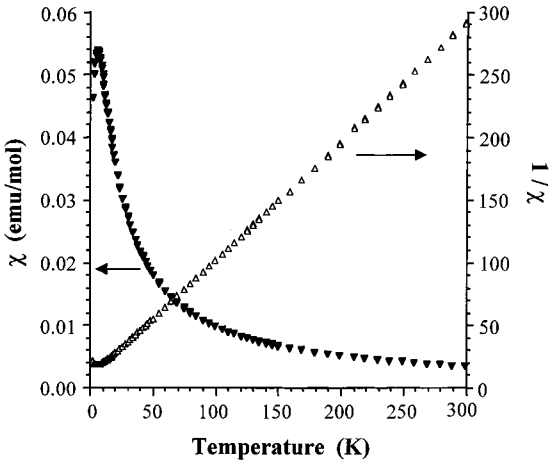

Figure 4. Temperature dependence of the molar and inverse molar susceptibilities of Sr_3PbNiO_6, at 40 kOe.

agreement with the theoretical spin-only value for octahedral Ni^{2+} (d^8, $t_{2g}^6e_g^2$, $S = 1$) of 2.83 μ_B. No magnetic frustration was observed, as the field-cooled and zero-field-cooled susceptibility vs temperature are identical at both field strengths (5 and 40 kOe) employed. A Curie−Weiss fit for $T > 20$K yielded the following constants: $C = 1.059(1)$ emu mol^{-1}, $\theta = -8.96(9)$ K, the latter indicating weak antiferromagnetic interactions between Ni^{2+} ions. Indeed, a relatively sharp antiferromagnetic transition is observed ($T_N = 6$ K), consistent with the negative Weiss constant.

Electronic structure calculations on $A_3A'BO_6$ magnetic systems where the spins are carried exclusively in the t_{2g} orbital set of the atom on the octahedral B site have recently supported earlier suggestions that these oxides do exhibit three-dimensional ordering,[17,41] which operates through a superexchange mechanism primarily via O···O contacts between *intra*- and *inter*chain polyhedra (i.e., Ni^{2+}—O···O—Ni^{2+}).[42] However, neither *intra*chain nor *inter*chain interactions dominate; their relative magnitude depends on the size of the nonmagnetic ion in the A′ site. When the radius of A′ ion in the chains is small compared to the A^{2+} cation between chains (r(A′)/$r(A^{2+}) < \sim 0.6$), superexchange via *intra*chain O···O contacts becomes the more important term. In Sr_3PbNiO_6, the e_g orbital set carries the spins; however, these couple *intra*- and *inter*chain similarly to the t_{2g} set, and the trend is still valid. The radius ratio of Pb^{4+} (C.N. = 6, $r = 0.78$ Å) to Sr^{2+} (C.N. = 8, $r = 1.26$ Å) is 0.57, implying a greater *intra*chain term. Both types of coupling are most likely present, and a more detailed investigation of the three-dimensional magnetic structure would be needed to clarify.

In conclusion, we have succeeded in incorporating lead into the $A_3A'BO_6$ family of pseudo-one-dimensional oxides. Sr_3PbNiO_6 offers the first example of trigonal prismatic Pb^{4+} as well as the first example of Ni^{2+} in the octahedral site in an $A_3A'BO_6$ oxide. The larger size of the Pb^{4+} ion relative to Ni^{2+} leads to an unprecedented "inverse" cation distribution in the metal−oxygen polyhedral chains. The compound shows Curie−Weiss behavior consistent with octahedral Ni^{2+} ($\mu_{eff} = 2.91\ \mu_B$) until antiferromagnetic ordering occurs at $T_N = 6$ K.

Acknowledgment. Financial support was provided by the National Science Foundation through grant DMR 9873570. We thank Dr. Charles Campana of Bruker AXS for collection of the single-crystal data.

Supporting Information Available: A complete listing of atomic parameters, isotropic and anisotropic displacement parameters, bond distances and angles, and F_o/F_c tables from the single crystal and solution, and detailed neutron diffraction refinement information. This material is available free of charge via the Internet at http://pubs.acs.org.

CM990360P

(40) (a) Takeda, Y.; Kanamaru, F.; Shimada, M.; Koizumi, M. *Acta Crystallogr. B* **1976**, *32*, 2464. (b) Takeda, Y.; Hashino, T.; Miyamoto, H.; Kanamaru, F.; Kume, S.; Koizumi, M. *J. Inorg. Nucl. Chem.* **1972**, *34*, 1599.

(41) Segal, N.; Vente, J. F.; Bush, T. S.; Battle, P. D. *J. Mater. Chem.* **1996**, *6*, 395.

(42) Lee, K.-S.; Koo, H.-J.; Whangbo, M.-H. *Inorg. Chem.* **1999**, *38*, 2199.